

Response to Reviewers

Comment on acp-2021-764

Anonymous Referee #2

Liu et al. presented a typical ozone pollution event study of a coastal city of southeast China for the exploration of AOC, OH reactivity, radical chemistry and ozone pollution mechanism with OBM-MCM method. The predominant oxidant for AOC, dominant contributor for OH reactivity, important source of ROx radical were examined, as well as the ozone formation regime sensitivity. Finally, the VOCs emission reduction were proposed for limiting the radical recycling and O₃ formation. Overall, the paper is appropriate for publication at ACP subject to the following concerns.

Response: Thank you very much for your exploratory and constructive advice. Here, we have carefully revised the manuscript.

Specific comments:

Even though this paper clarifies several important characteristics and mechanism of the ozone pollution for a selected case, the representativeness for a short period and the specific location seems not to be abroad of interests. I would like to suggest the authors can enhance the significance of the findings for the readership.

Response: We thank the reviewer for the comments which are helpful for us to improve the paper. We have further revised the manuscript accordingly, and hope meet with approval.

Regarding to the location, the authors considered the site shows a relatively low O₃ precursors and complex meteorological conditions. However, no evidence was found for the comparison of levels of O₃ precursors, and also the impacts of complex meteorological conditions were not well discussed. These may be improved via, e.g.: (1) comparative study on the non-low levels of O₃ precursors case for the ozone pollution; (2) the impacts of change of meteorological conditions (not only the synoptic situation) on the ozone pollution.

Response: Thanks for your suggestion. Based on your suggestions, we made the following changes.

(1)

The comparison of NO, NO₂ and total VOCs levels in cities between China and other countries is listed in Table 1. The comparison indicated relatively low O₃ precursor emissions in our observation site. And the detailed comparative discussion on the non-

low levels of O₃ precursors case for the ozone pollution was also added to the revised manuscript.

“In a coastal city of Southeast China, the concentrations of O₃ precursors were higher than those in remote sites and background, but lower than those in most of urban and suburban areas, even lower than those in rural regions (Table S1). In a word, O₃ precursor emissions in our observation site were relatively low.”

“The concentration of TVOCs in Xiamen (17.2±4.8 ppbv) was lower than that in the developed areas with large anthropogenic emissions (i.e., Beijing (41.2 ppbv), Lanzhou (45.3 ppbv), Wuhan (30.2 ppbv), Chengdu (36.0 ppbv), Hong Kong (26.9 ppbv), Los Angeles (41.3 ppbv) and Tokyo (43.4 ppbv), comparable to some urban with low pollution emissions (i.e., Wuhan (30.2 ppbv), Chengdu (36.0 ppbv), Hong Kong (26.9 ppbv), Los Angeles (41.3 ppbv) and Tokyo (43.4 ppbv)), but was higher than that at the background and remote sites (i.e., Mt. Wuyi (6.1 ppbv) and Mt. Waliguan (2.6 ppbv)) (Table S1).”

Table S1 Comparison of NO, NO₂ and total VOCs levels in cities between China and other countries (Unit: ppbv).

Location	NO ₂	NO	VOCs	Site category	Observation periods	Reference
Xiamen	15.4	1.4	17.2	Urban	Sep. 2019 (episode)	This study
Beijing	16.8	2.1	44.2	Urban		Liu et al., 2021b
Wuhan	17.5	3.2	30.2	Urban	Summer 2018 (episode)	Liu et al., 2021b
Lanzhou	15.8	2.9	45.3	Urban		Liu et al., 2021b
Shanghai	14.2	3.38	25.3	Urban	Jun. 2019 (episode)	Zhu et al., 2020
Chengdu	39.0	3.6	36.0	Urban	Jul. 2017 (episode)	Yang et al., 2020
Los Angeles	-	-	41.3	Urban	May. to Jun. 2010	Warneke et al., 2012
London	-	-	22.1	Urban	1998–2008	Von Schneidmesser et al., 2010
Tokyo	-	-	43.4	Urban	2003–2005	Hoshi et al., 2008
Beijing	11.5	4.8	28.1	Suburban	Aug. 2018	Yang et al., 2021
Hong Kong	25.0	14.0	26.9	Suburban	Aug. to Nov. 2013	Wang et al., 2018
Chengdu	11.4	8.0	28.0	Suburban	Summer 2019	Yang et al., 2021a
Qingdao	16.7	1.6	7.6	Rural	Oct. to Nov. 2019	Liu et al., 2021a
The Pearl River Delta	39.9	4.2	38.0	Rural	Octo. to Nov. 2014	He et al., 2019
Hong Kong	12.2	1.9	10.9	Regional background	Aug. to Dec. 2012	Li et al., 2018
Mt. Wuyi	-	-	4.7	Background	Dec. 2016	Hong et al., 2019
Mt. Tai	-	-	8.8	Background	Jun. 2006	Suthawaree et al., 2010
Mt. Waliguan	-	-	2.6	Remote region	Jul. to Aug. 2003	Xue et al., 2013

Note: “-” means that the data was not mentioned in the relevant studies.

(2)

We strongly agree with your suggestions of strengthening the analysis of meteorological conditions. During the observation periods, Xiamen was affected by

various meteorological conditions, such as typhoon and the West Pacific Subtropical High (WPSH) accompanied by temperature inversion phenomenon, thus we focused on the analysis of meteorological conditions and ignored the conventional analysis of other meteorological parameters (wind speed (WS), air temperature (T), pressure (P), relative humidity (RH), and photolysis rate constants). Hence, we used the Generalized Additive Model (GAM) to study the influencing factors on O₃ pollution. GAM model has been widely used in O₃ pollution research, and can deal with the complex nonlinear relationship between O₃ and its influencing factors effectively (Hua et al., 2021; Ma et al., 2020). The detailed discussion was shown in the manuscript of Section 3.3.2, and the main revisions are as follows.

“Favorable meteorological conditions significantly affected the formation and accumulation of O₃, and we chose five meteorological parameters (i.e. UV, T, RH, P and WS) to quantify the complex nonlinear relationships between O₃ and its influencing factors based on a generalized additive model (GAM) (Hua et al., 2021). Table S3 showed that the factors had significant non-linear impacts on O₃ concentration changes at the level of P-value<0.01 and degrees of freedom>1, indicating that each influencing factor has statistical significance as an explanatory variable. According to the F-values reflecting the importance of the influencing factors, the orders of the explanatory variables were RH (40.1) > WS (26.9) > T (10.9) > P (3.9) > UV (3.0). Response curves of O₃ concentration to explanatory factors are presented in Fig. 13. The O₃ concentration showed a remarkable upward trend until the UV increased to 17 W·m⁻², then changed little with the fluctuation of UV (Fig. 13a). In previous studies, UV had a significant positive correlation with O₃ concentrations (Ma et al., 2020), and these results showed the regional transport impacts on O₃ formation in our study. The RH and T had negative and positive correlations with O₃ concentrations, respectively (Fig. 13b and Fig. 13c). The increase of wind speed was favorable for O₃ regional transport (Fig. 13d). The influence of atmospheric pressure on O₃ seemed to be irregular and minor, which could be ignored (Fig. 13e).”

Table S3 Estimated degree of freedom (Edf), degree of reference (Ref. df), P-value, F-value, deviance explained (%), adjusted R² for the smoothed variables (including UV, T, RH, P, and WS) in the GAM model.

Smoothed variables	^a Edf	^a Ref.df	^b F	^c P-value	^d Adjust R ²	^e Deviance explained (%)
UV (W·m ⁻²)	3.1	3.8	3.0	0.0	0.0	5.4
T (°C)	5.3	6.5	10.9	0.0	0.2	24.1
RH (%)	2.9	3.6	40.1	0.0	0.4	38.9
WS (m·s ⁻¹)	2.9	3.6	26.9	0.0	0.3	29.3
P (hPa)	6.9	8.0	3.9	0.0	0.1	13.4

Note: ^a The degree of freedom (edf, ref.df) of the explanatory variable is 1, indicating the linear relationships between the explanatory variable and the response variable, and a non-linear relationship is shown when the degree>1; ^b a high F-value indicates the great importance of the influencing factor; ^c the P-value is used to judge the significance of the model result; ^d the adjusted

R^2 is the value of the regression square ranging from 0 to 1; ° the deviance explained represents the fitting effect.

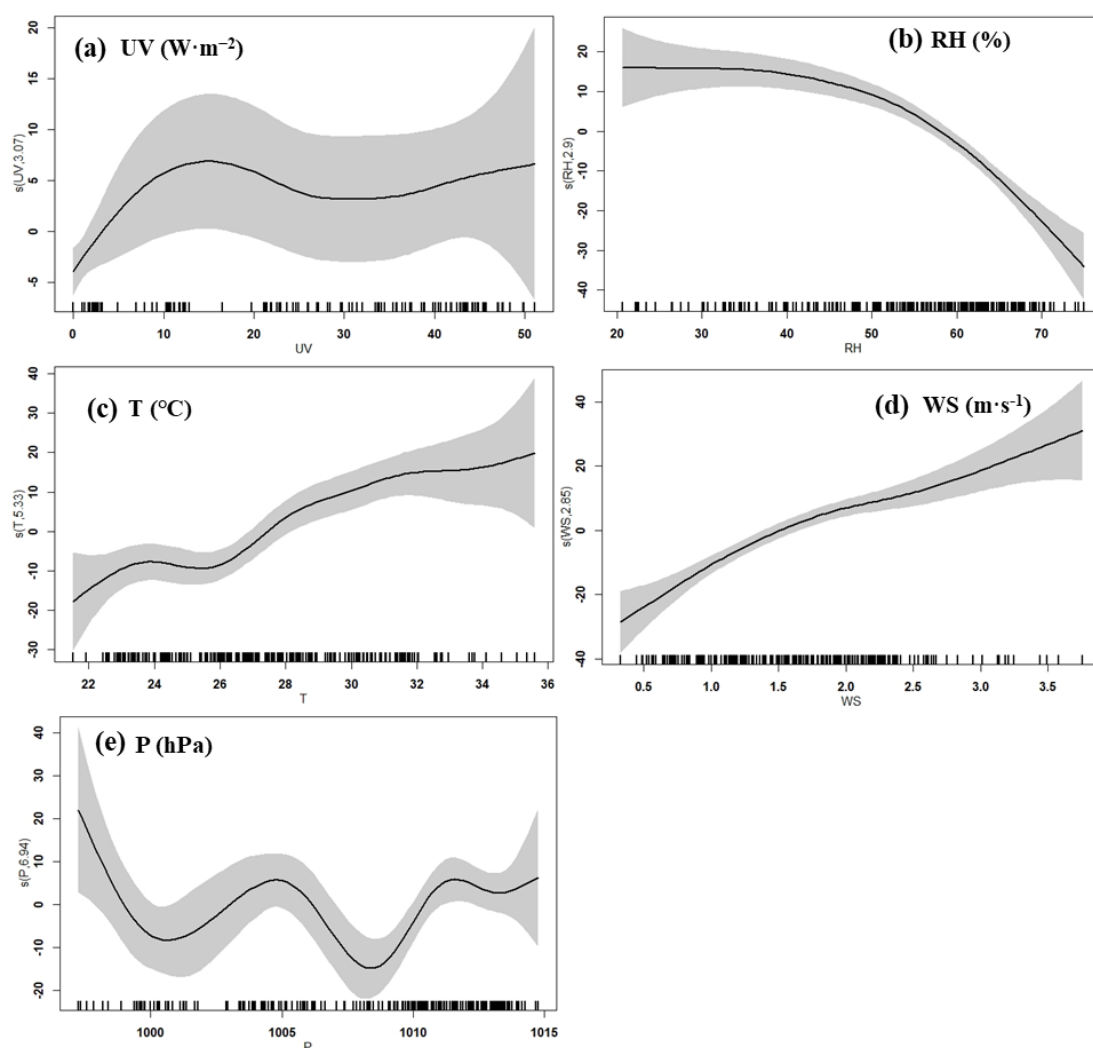


Figure 13. Response curves in GAM model of O₃ concentration to changes in (a) ultraviolet radiation (UV), (b) relative humidity (RH), (c) temperature (T), (d) wind speed (WS), and (e) pressure (P). The y-axis is the smoothing function values. The x-axis is the influencing factor; the vertical short line represents the amount of data; the shaded area around the solid line indicates the 95% confidence interval of O₃ concentration.

I could not find the observed HCHO data in the paper, which is very important for the observation constrained modeling, and further discussion on the radical sources and evaluation of the highest OFP species.

Response: Thank you for your suggestions. We strongly agree with this idea that HCHO is very important for observation constrained modeling.

The gas chromatography-mass spectrometer (GC-FID/MS, TH-300B, Wuhan, CN)

used for atmospheric VOCs concentrations monitoring cannot detect HCHO in this study. When the HCHO concentrations were not observed, the concentrations could be locally and reasonably calculated by the model according to the other observed pollutants of O₃ precursors (Table 2). Some studies exploring the O₃ formation mechanism based on OBM model also did not observe HCHO data (Chen et al., 2020, Liu et al., 2021; Li et al., 2018; Wang et al., 2020). Meanwhile, we strongly agree with your idea and realized the importance of HCHO in O₃ formation, hence our team improved the monitoring of *Atmospheric Formaldehyde Online Analyzer* and *Chemical Ionization Mass Spectrometry (CIMS)* in May 2021. A more optimized and complete monitoring system is also the future optimization goal of our model.

Meanwhile, the index of agreement (IOA) can be used to judge the reliability of the model simulation results, and its equation is (Liu et al., 2019).

$$IOA = 1 - \frac{\sum_{i=1}^n (O_i - S_i)^2}{\sum_{i=1}^n (|O_i - \bar{O}| + |S_i - \bar{O}|)^2} \quad (4)$$

where S_i is simulated value, O_i represents observed value, \bar{O} is the average observed values, and n is the sample number. The IOA range is 0-1, and the higher the IOA value is, the better agreement between simulated and observed values is. In many studies, when IOA ranges from 0.68 to 0.89 (Wang et al., 2018a), the simulation results are reasonable, and the IOA in our research is 0.80. The hourly simulated and observed O₃ during the observation periods at the study site in Figure R1 showed that the performance of the OBM-MCM model was reasonably acceptable.

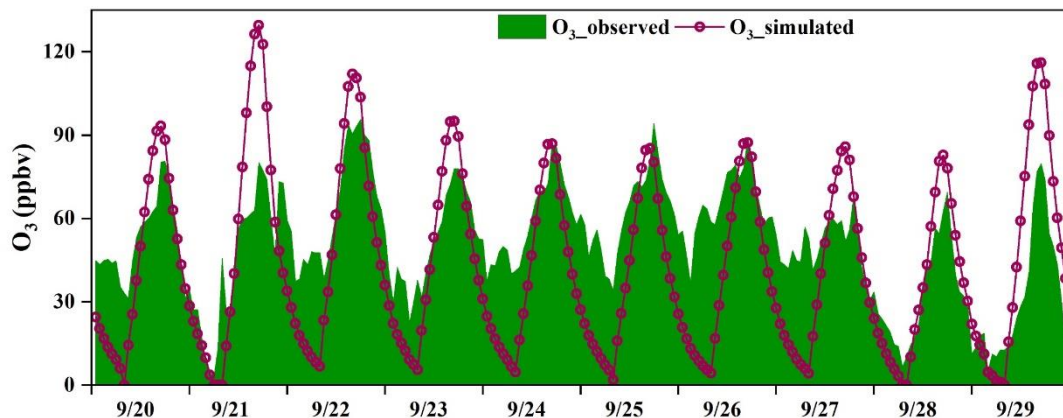


Figure R1. The hourly simulated and observed O₃ during the observation periods at the study site.

The OFP results had relatively great errors brought by the missing data of HCHO. In this study, we only calculated the OFP values briefly and did not analyze them in-depth, which could not help my analysis well and even confuse readers. Anymore, the OH reactivities and RIRs can better reflect the importance of its precursors for O₃ formation. Hence, we think it is a better choice to delete the analysis of OFP from the revised manuscript, which can help readers better understand the full text.

OBM modeling: Please specify the setting of dry deposition velocity.

Response: Thanks for your suggestion. The specific setting of dry deposition velocity was shown in the supporting information (Table S2).

Table S2. Dry deposition velocity (cm s^{-1}) for chemical species (Zhang et al., 2003).

Symbol	Name	dry deposition velocity
O ₃	Ozone	0.6
NO ₂	Nitrogen dioxide	0.6
HONO	Nitrous acid	1.9
HNO ₃	Nitric acid	4.7
HNO ₄	Pernitric acid	3.3
NH ₃	Ammonia	1
SO ₂	Sulphur dioxide	0.8
H ₂ SO ₄	Sulphuric acid	1.1
H ₂ O ₂	Hydrogen peroxide	1.2
PAN	Peroxyacetyl nitrate	0.4
PPN	Peroxypropyl nitrate	0.4
APAN	Aromatic acyl nitrate	0.5
MPAN	Peroxy methacrylic nitric anhydride	0.3
HCHO	Formaldehyde	0.9
MCHO	Acetaldehyde	0.2
PALD	C3 Carbonyls	0.2
C4A	C4-C5 Carbonyls	0.2
C7A	C6-C8 Carbonyls	0.2
ACHO	Aromatic carbonyls	0.2
MVK	Methyl-vinyl-ketone	0.2
MACR	Methacrolein	0.2
MGLY	Methylglyoxal	0.2
MOH	Methyl alcohol	0.7
ETOH	Ethyl alcohol	0.6
POH	C3 alcohol	0.5
CRES	Cresol	0.2
FORM	Formic acid	1.4
ACAC	Acetic acid	1.1
ROOH	Organic peroxides	0.6
ONIT	Organic nitrates	0.4
INIT	Isoprene nitrate	0.3

Line 47, “&” may be not the suitable format for the text. Btw, here the authors want to indicate the “temporal and spatial distribution” of what? Ozone concentration? or precursors? Please clarify it.

Response: As you suggested, we have clarified the temporal and spatial distribution, and the main revisions are as follows.

“O₃ formation is affected by multiple factors such as O₃ precursor speciation or level, atmospheric oxidation capacity, meteorological conditions and regional transport.”

Line 139-148, Please list the relevant reaction and reaction rates in the Eq. 1 to Eq. 3, at least in the Supplementary.

Response: Thanks for your suggestion. The relevant reaction and reaction rates were listed in Table 1, and the main revisions are as follows.

“Table 1 shows the production and destruction reactions and relevant reaction rates of O₃ in our study. The production rate of O₃ (P(O₃)) includes RO₂+NO (R1) and HO₂+NO reactions (R2, Eq. 1), and the destruction of O₃ (D(O₃)) involves reactions of O₃ photolysis (R3), O₃+OH (R4), O₃+HO₂ (R5), NO₂+OH (R6), O₃+VOCs (R7), and NO₃+VOCs (R8, Eq. 2). The net O₃ production rate (Pnet(O₃)) is calculated by P(O₃) minus D(O₃) as equation 3.”

Table 1 Simulated production and destruction reactions and relevant reaction rates of O₃.

Reactions	Reaction rates	Number
O₃ production pathways-P(O₃)		
RO ₂ +NO→RO+NO ₂	$2.7 \times 10^{-12} \times \text{EXP}(360/T)$	R1
HO ₂ +NO→OH+NO ₂	$3.45 \times 10^{-12} \times \text{EXP}(270/T)$	R2
O₃ destruction pathways-D(O₃)		
O ₃ +hν→O ¹ D+O ₂	JO ¹ D	R3a
O ¹ D+H ₂ O→OH	2.14×10^{-10}	R3b
O ₃ +OH→HO ₂	$1.70 \times 10^{-12} \times \text{EXP}(-940/T)$	R4
O ₃ +HO ₂ →OH	$2.03 \times 10^{-16} \times (T/300)^{4.57} \times \text{EXP}(693/T)$	R5
NO ₂ +OH→HNO ₃	$3.2 \times 10^{-30} \times 9.7 \times 10^{18} \times P/T \times (T/300)^{-4.5} \times 3.0^{11} \times 10^{\log_{10}(0.41)} / (1 + (\log(3.2^{-30} \times 9.7 \times 10^{18} \times P/T \times (T/300)^{-4.5} \times 3.0^{11} \times 10^{\log_{10}(0.41)} / ((0.75 - 1.27 \times (\log_{10}(0.14))^2) / (3.2^{-30} \times 9.7 \times 10^{18} \times P/T \times (T/300)^{-4.5} + 3.0^{-11})))$	R6
O ₃ +VOCs→Carbonyls+Criegee biradical	Kcons.1	R7
NO ₃ +VOCs→RO ₂	Kcons.2	R8

Note: The reaction rates of Kcons.1 and Kcons.2 were constant. There were around 700 reactions of VOCs+NO₃/O₃, and the relevant reaction rates were different constants, which can be obtained from this website <http://mcm.leeds.ac.uk/MCM/>.

Line 234-239, High AOC were calculated for the ozone pollution episode in this study, which is significantly higher than those at Hongkong, Shanghai, etc. However, as stated in the introduction, the AOC levels in the polluted regions are much higher than those

at the background sites or remote regions. Does it mean that this site can be classified as a polluted one? And contradict to that non-low level of precursors? The authors should discuss carefully what are the main reasons causing the high AOC in this study.

Response: Thanks for your suggestion. We apologize for the confusion caused by the incorrect AOC calculation and inappropriate comparison of AOC among different cities in my study.

The AOC is calculated as the sum of oxidation rates of various primary pollutants (CO, NO_x, VOCs, etc.) by the major oxidants (i.e., OH, O₃, NO₃), which did not list the types of VOCs in detail. In fact, the species of VOCs in AOC calculation mainly include alkanes, alkenes, aromatics and OVOCs, while we computed AOC using many VOCs that should not be considered in AOC calculation, so that the AOC levels in our study were overestimated. We recalculated AOC (Fig. 3) and have corrected it in the manuscript. After comparison of the recalculated AOC, the concentrations of O₃ precursors in Xiamen were lower than those in Hong Kong and Shanghai we mentioned, but the AOC levels in our study were comparable to or even lower compared with the AOC in Hong Kong and Shanghai. According to the AOC definition, the key factors to quantify AOC are processes and rates of species being oxidized in the atmosphere (Liu et al., 2021c). Hence, the factors of photolysis rate, meteorological conditions, pollutant concentrations and regional transport would influence the AOC levels, and we cannot think the high AOC value means the polluted levels of the regions. When we compare the AOC among different sites, we should compare the daily maximum AOC and also analyze other relevant information, such as site category, solar radiation, pollutant concentrations. As Table R1 shown, although the levels of O₃ precursors in these urban sites were higher than those in Xiamen, the photolysis rates in these cities were lower than those in Xiamen. The detailed discussions were shown in the manuscript.

Table R1 Comparison of NO, NO₂, total VOCs (ppbv), AOC (molecules cm⁻³ s⁻¹) and J(NO₂) levels in Xiamen, Shanghai and Hong Kong.

Location	NO ₂	NO	VOCs	Site category	AOC	Maximum AOC	J(NO ₂) (10 ⁻³ s ⁻¹)	Maximum J(NO ₂)	Reference
Xiamen	15.4	1.4	17.2	Urban	6.7×10 ⁷	1.3×10 ⁸	3.5	11.1	This study
Shanghai	14.2	3.4	25.3	Urban	3.9×10 ⁷	1.0×10 ⁸	2.8	8.0	Liu et al., 2020
Hong Kong	-	-	32.7	Urban	6.3×10 ⁷	1.3×10 ⁸	-	6.0	Xue et al., 2016
Hong Kong	12.2	1.9	10.9	Regional background	1.6×10 ⁷	6.2×10 ⁷	2.3	9.3	Li et al., 2018

Note: “-” means that the data was not mentioned in the relevant studies.

“The atmospheric oxidation capacity reflects the essential driving force in tropospheric chemistry, and plays an important place in the loss rates of primary components and production rates of secondary pollutants, thus the key factors to quantify AOC are processes and rates of species being oxidized in the atmosphere (Elshorbany et al., 2008). The atmospheric conditions (such as photolysis rate, meteorology, pollutant

concentrations and regional transport) together influence the AOC levels, and the AOC levels in the polluted urban regions are generally much higher than those at the background sites or remote regions due to the dominant limited factor for the significant differences of pollutant concentrations.”

3.1 Overview of observations

“Our previous study showed that particulate pollution was slight in Xiamen, which could affect solar radiation by light-absorbing component, and the concentrations of particulate matter had not exceeded the National Ambient Air Quality Standard (Class II: $75 \mu\text{g} \cdot \text{m}^{-3}$) for a whole year (Hu et al., 2021; Deng et al., 2020). Therefore, solar radiation intensity and $J(\text{NO}_2)$ were strong, compared to those of the Yellow River Delta (Chen et al., 2020), Shanghai (Zhu et al., 2020) and Hong Kong (Xue et al., 2016).”

3.2.1 Atmospheric oxidation capacity (AOC)

“In this study, the average daytime AOC was 6.7×10^7 molecules $\text{cm}^{-3} \text{s}^{-1}$, and the daily maximum AOC was 1.3×10^8 molecules $\text{cm}^{-3} \text{s}^{-1}$, which was higher than those at rural sites with much low pollution emissions in Berlin (1.4×10^7 molecules $\text{cm}^{-3} \text{s}^{-1}$) and regional background in Hong Kong (6.2×10^7), but lower than that in polluted cities, such as Santiago (3.2×10^8 molecules $\text{cm}^{-3} \text{s}^{-1}$), due to the main limited factor of the significant differences of pollutant concentrations among different sites (Li et al., 2018; Xue et al., 2016; Geyer et al., 2001; Zhu et al., 2020). In some urban regions, the concentrations of air pollutants were higher than those in Xiamen, but their AOC levels (Hong Kong: 1.3×10^8 molecules $\text{cm}^{-3} \text{s}^{-1}$; Shanghai: 1.0×10^8 molecules $\text{cm}^{-3} \text{s}^{-1}$) were comparable to or even lower compared with the AOC in Xiamen, which could be attributed to the relatively high solar radiation (Detailed descriptions showed in Section 3.1).”

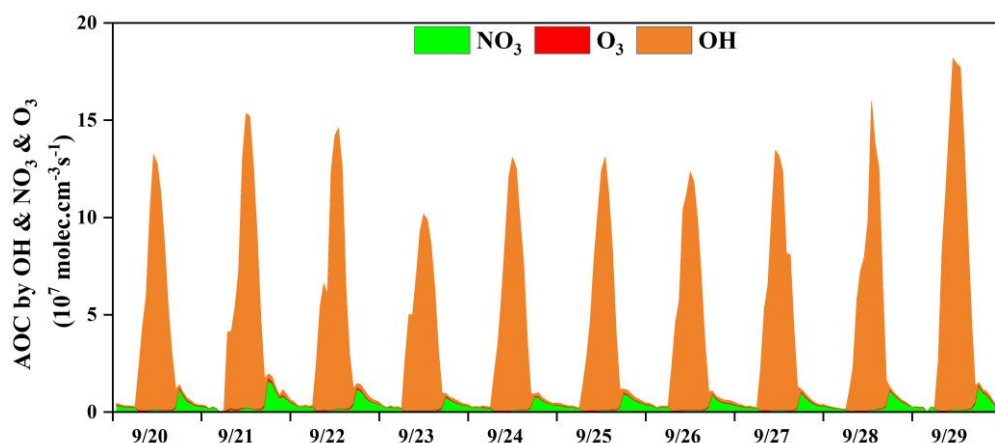


Figure 3. Time series of the model-calculated Atmospheric Oxidation Capacity (AOC) in Xiamen during 20-29 Sep. 2019.

Line 354-358, the classification of VOCs can be indicated in the Table 2.

Response: Thanks for your suggestion. The relevant classification of VOCs was indicated in the Table 2.

Table 2. Measured VOCs concentrations during 20-29 Sep. 2019 in Xiamen (Units: pptv), and the classification of VOCs were used and introduced in Section 3.3.

Chemicals	Classification	Mean±SD	Chemicals	Classification	Mean±SD
Aromatics		2131±1236	Alkanes		6970±2325
toluene	RAROM/AHC	995±632	ethane	LRHC/AHC	1552±342
m/p-xylene	RAROM/AHC	392±326	propane	LRHC/AHC	1546±608
benzene	LRHC/AHC	236±95	iso-pentane	C4HC/AHC	930±316
o-xylene	RAROM/AHC	154±121	n-butane	C4HC/AHC	844±365
ethylbenzene	RAROM/AHC	138±94	n-dodecane	C4HC/AHC	618±101
styrene	RAROM/AHC	76±65	iso-butane	C4HC/AHC	494±201
1,2,4-trimethylbenzene	RAROM/AHC	75±37	n-pentane	C4HC/AHC	254±157
m-ethyltoluene	RAROM/AHC	16±11	n-hexane	C4HC/AHC	134±184
p-ethyltoluene	RAROM/AHC	10±6	3-methylhexane	C4HC/AHC	116±93
iso-propylbenzene	RAROM/AHC	5±3	n-heptane	C4HC/AHC	104±78
1,3,5-trimethylbenzene	RAROM/AHC	8±6	3-methylpentane	C4HC/AHC	82±48
o-ethyltoluene	RAROM/AHC	8±5	2-methylhexane	C4HC/AHC	67±38
1,2,3-trimethylbenzene	RAROM/AHC	7±5	2-methylpentane	C4HC/AHC	56±46
n-propylbenzene	RAROM/AHC	7±4	2,3-dimethylbutane	C4HC/AHC	54±33
Halocarbons		1951±572	cyclohexane	C4HC/AHC	42±15
dichloromethane	AHC	998±392	n-undecane	C4HC/AHC	33±35
1,2-dichloroethane	AHC	499±210	n-octane	C4HC/AHC	24±15
chloromethane	AHC	294±75	n-nonane	C4HC/AHC	15±13
1,2-dichloropropane	AHC	88±34	2,2-dimethylbutane	C4HC/AHC	15±7
bromomethane	AHC	47±23	n-decane	C4HC/AHC	14±11
trichloroethene	AHC	15±6	Alkenes		1205±464
1,4-dichlorobenzene	AHC	9±3	ethene	Alkenes/AHC	671±361
OVOCs		4246±1263	propene	Alkenes/AHC	207±116
acetone	AHC	2802±750	isoprene	BHC	171±232
2-butanone	AHC	799±430	trans-2-pentene	Alkenes/AHC	105±62
2-propanol	AHC	343±283	1-butene	Alkenes/AHC	16±21
2-methoxy-2-methylpropane	AHC	169±97	cis-2-butene	Alkenes/AHC	12±12
acrolein	AHC	66±22	1-pentene	Alkenes/AHC	10±7
4-methyl-2-pentanone	AHC	16±15	1,3-butadiene	Alkenes/AHC	8±7
2-hexanone	AHC	12±3	trans-2-butene	Alkenes/AHC	4±4
			Acetylene	LRHC/AHC	674±290

Fig. 11, The Rtran was determined by the difference of Rmeas and Rchem. So my main concern is that how about the accuracy of Rtran? At least, I think it include the considerable uncertainties of Rchem. The inference about transport amount need be

more cautious. Also no evidence provided can prove the northerly air flow is ozone polluted. Secondly, the authors explained why the two regular O_3 important phenomenon with positive R_{tran} happened. However, why did negative R_{tran} observed around noontime every day?

Response: Thanks for your suggestion. We strongly agree that there were uncertainties in the model simulation.

Firstly, the observation data of the gaseous pollutants (i.e., O_3 , CO, NO, NO_2 , HONO, SO_2 , and VOCs), meteorological parameters (i.e., T, P, and RH), and photolysis rate constants ($J(O^1D)$, $J(NO_2)$, $J(H_2O_2)$, $J(HONO)$, $J(HCHO)$, and $J(NO_3)$) were input into the OBM-MCM model as constraints to realize model simulation localization. Secondly, the model performance of AOI as mentioned in the second question was reasonably acceptable in this study. Hence, the simulated R_{chem} values could well reflect the actual local atmospheric photochemistry.

The in-situ ozone concentration change is a result of both physical and chemical processes. The O_3 concentration change rate (R_{meas}) can be determined by the derivative of the observed O_3 concentration. The difference between R_{meas} and R_{chem} is caused by physical processes, including horizontal and/or vertical transportation, deposition, and so on, and many studies showed that the impacts of deposition were minor. Anymore, the changes of near-surface winds were corresponding to the variation of the R_{trans} in our study. In some relevant studies, their results also suggested that this method can capture the variations in physical processes, thereby, this calculation method could reasonably quantify the contributions of regional transport (Zhang et al., 2021; Xue et al., 2014; Tan et al., 2018; Chen et al., 2020).

About the northerly O_3 polluted airflow, we revised this sentence as “the northerly airflow with high O_3 or its precursors from an industrial city adjacent to Xiamen of Quanzhou or polluted regions of Yangtze River Delta”. Figure R1 shows the 72 h back trajectories in spring and autumn, when the northerly air masses appear frequently in our observation site. In the four pictures of Fig. R1, we could find that the air masses coming from the north carried higher O_3 concentration than air masses coming from other directions, attributing to economic and industrially developed areas in the north direction of Xiamen.

About the negative R_{tran} observed around noontime:

The maximum daily value of O_3 at this observation site generally appeared at around 15:00 LT without regional transport, and the values appeared at around 17:00 LT when there was significant regional transport. In Figure 11, we found that the O_3 concentrations still showed two peaks at around 15:00 and 17:00 LT, and O_3 concentrations rose slowly, or even decreased firstly and then increased between the two peaks. When the O_3 concentrations rose slowly or decreased, the R_{meas} values would be close to 0 or less than 0, which were less than the R_{chem} values (R_{chem}

values were positive until sunset). Under these circumstances, the local photochemical production kept producing O₃, while O₃ concentrations remained the same or even decreased, which could be attributed to the favorable atmospheric conditions in diluting pollutants (O₃ export). In conclusion, the negative Rtran observed around noontime is a phenomenon caused by favorable atmospheric diffusion conditions, which also happened in other regions (Beijing, Shanghai, Guangzhou, Lanzhou, Chengdu and the Yellow River Delta region) (Zhang et al., 2021; Xue et al., 2014; Tan et al., 2018; Chen et al., 2020). The second peak of the Rmeas showing the “M” trend during the daytime was mainly caused by regional transport. And the main revisions in the manuscript are as follows.

“The O₃ export was remarkable at around 10:00-16:00, indicating the potential impacts on air quality in downwind areas. Generally, the maximum daily value of O₃ at this observation site appeared at around 15:00 LT without regional transport (Wu et al., 2019). In Figure 11, we found that the O₃ concentrations showed two peaks at around 15:00 and 17:00 LT, and O₃ concentrations rose slowly, or even decreased firstly and then increased between the two peaks. Under these circumstances, the local photochemical production kept producing O₃, but the decreased O₃ concentrations could be attributed to the favorable atmospheric conditions in diluting pollutants (O₃ export).”

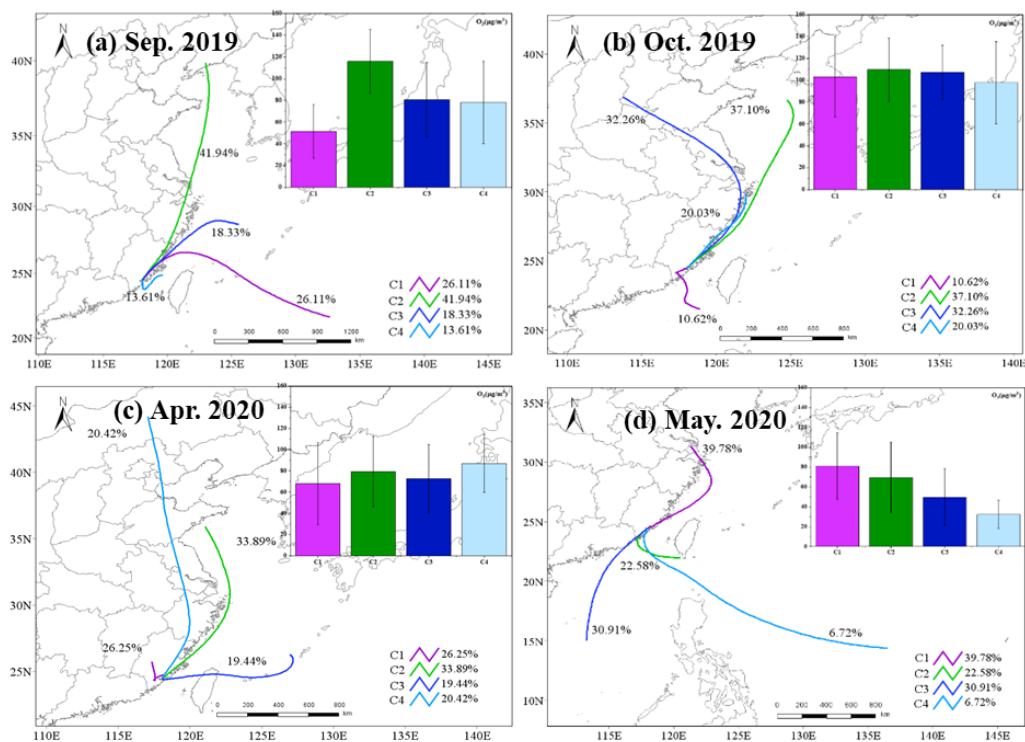


Figure R1. Cluster results of air mass trajectories, relative contributions of O₃ concentrations of each air mass by month.

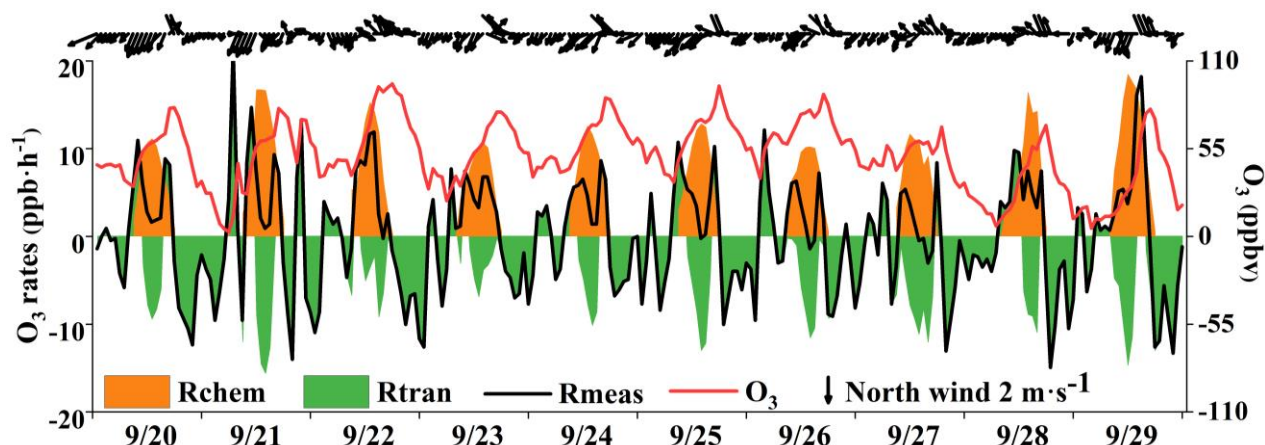


Figure 11. O₃ accumulation and contributions from local photochemical production and regional transport, and Rchem, Rtran, and Rmeas in figure caption represent local O₃ photochemical production, regional transport and observed O₃ formation rate, respectively.

The English may need be improved, e.g.

Line 50, “control factors” to “controlling factors”.

Line 53, “destruction rates” to “loss rates”.

Line 57, “oxidative” to “oxidation”.

etc.

Response: We’re sorry for the inappropriate expressions. Thanks for your suggestion, and we have invited native speakers in related fields to polish the manuscript.

Reference:

Chen, T., Xue, L., Zheng, P., Zhang, Y., Liu, Y., Sun, J., Han, G., Li, H., Zhang, X., Li, Y., Li, H., Dong, C., Xu, F., Zhang, Q., and Wang, W.: Volatile organic compounds and ozone air pollution in an oil production region in northern China, *Atmospheric Chemistry and Physics*, 20, 7069-7086, 10.5194/acp-20-7069-2020, 2020.

Li, Z., Xue, L., Yang, X., Zha, Q., Tham, Y. J., Yan, C., Louie, P. K. K., Luk, C. W. Y., Wang, T., and Wang, W.: Oxidizing capacity of the rural atmosphere in Hong Kong, Southern China, *Sci Total Environ*, 612, 1114-1122, 10.1016/j.scitotenv.2017.08.310, 2018.

Liu, Y., Shen, H., Mu, J., Li, H., Chen, T., Yang, J., Jiang, Y., Zhu, Y., Meng, H., Dong, C., Wang, W., and Xue, L.: Formation of peroxyacetyl nitrate (PAN) and its impact on ozone production in the coastal atmosphere of Qingdao, North China, *Sci Total Environ*, 778, 146265, 10.1016/j.scitotenv.2021.146265, 2021a.

Zhang L , Brook J R , Vet R . A revised parameterization for gaseous dry deposition in air-quality models. *Atmos. Chem. Phys.*, 3(2), 2067-2082, 2003.

Liu, X., Lyu, X., Wang, Y., Jiang, F., and Guo, H.: Intercomparison of O₃ formation and radical chemistry in the past decade at a suburban site in Hong Kong, *Atmos. Chem. Phys.*, 19, 5127-5145, 10.5194/acp-19-5127-2019, 2019.

Wang, Y., Guo, H., Zou, S., Lyu, X., Ling, Z., Cheng, H., and Zeren, Y.: Surface O₃ photochemistry over the South China Sea: Application of a near-explicit chemical mechanism box model, *Environ Pollut*, 234, 155-166, 10.1016/j.envpol.2017.11.001, 2018a.

Wang, M., Chen, W., Zhang, L., Qin, W., Zhang, Y., Zhang, X., and Xie, X.: Ozone pollution characteristics and sensitivity analysis using an observation-based model in Nanjing, Yangtze River Delta Region of China, *J Environ Sci (China)*, 93, 13-22, 10.1016/j.jes.2020.02.027, 2020.

Tan, Z., Lu, K., Jiang, M., Su, R., Dong, H., Zeng, L., Xie, S., Tan, Q., and Zhang, Y.: Exploring ozone pollution in Chengdu, southwestern China: A case study from radical chemistry to O₃-VOC-NO_x sensitivity, *Sci Total Environ*, 636, 775-786, 10.1016/j.scitotenv.2018.04.286, 2018.

Xue, L. K., Wang, T., Gao, J., Ding, A. J., Zhou, X. H., Blake, D. R., Wang, X. F., Saunders, S. M., Fan, S. J., Zuo, H. C., Zhang, Q. Z., and Wang, W. X.: Ground-level ozone in four Chinese cities: precursors, regional transport and heterogeneous processes, *Atmos. Chem. Phys.*, 14, 13175-13188, 10.5194/acp-14-13175-2014, 2014.

Zhang, Y., Xue, L., Carter, W. P. L., Pei, C., Chen, T., Mu, J., Wang, Y., Zhang, Q., and Wang, W.: Development of Ozone Reactivity Scales for Volatile Organic Compounds in a Chinese Megacity, *ACP*, 10.5194/acp-2021-44, 2021.

Liu, Z., Wang, Y., Hu, B., Lu, K., Tang, G., Ji, D., Yang, X., Gao, W., Xie, Y., Liu, J., Yao, D., Yang, Y., and Zhang, Y.: Elucidating the quantitative characterization of atmospheric oxidation capacity in Beijing, China, *Sci Total Environ*, 771, 145306, 10.1016/j.scitotenv.2021.145306, 2021a.

Liu, X., Guo, H., Zeng, L., Lyu, X., Wang, Y., Zeren, Y., Yang, J., Zhang, L., Zhao, S., Li, J., and Zhang, G.: Photochemical ozone pollution in five Chinese megacities in summer 2018, *Sci Total Environ*, 149603, 10.1016/j.scitotenv.2021.149603, 2021b.

Yang, X., Wu, K., Wang, H., Liu, Y., Gu, S., Lu, Y., Zhang, X., Hu, Y., Ou, Y., Wang, S., and Wang, Z.: Summertime ozone pollution in Sichuan Basin, China: Meteorological conditions, sources and process analysis, *Atmos. Environ.*, 226, 117392, 10.1016/j.atmosenv.2020.117392, 2020.

Warneke, C., Gouw, J.A., Holloway, J.S., Peischl, J., Ryerson, T.B., Atlas, E., Blake, D., Trainer, M., Parrish, D.D.: Multiyear trends in volatile organic compounds in Los Angeles, California: five decades of decreasing emissions. *J. Geophys. Res.-Atmos.* 117 (D21). <http://dx.doi.org/10.1029/2012JD017899>, 2012.

Von Schneidemesser, E., Monks, P.S., Plass-Duelmer, C.: Global comparison of VOC and CO observations in urban areas. *Atmos. Environ.* 44 (39), 5053–5064, 2010.

Hoshi, J.Y., Amano, S., Sasaki, Y., Korenaga, T.: Investigation and estimation of emission sources of 54 volatile organic compounds in ambient air in Tokyo. *Atmos. Environ.* 42 (10), 2383–2393, 2008.

Wang, H., Lyu, X., Guo, H., Wang, Y., Zou, S., Ling, Z., Wang, X., Jiang, F., Zeren, Y., Pan, W., Huang, X., and Shen, J.: Ozone pollution around a coastal region of South China Sea: interaction between marine and continental air, *Atmos. Chem. Phys.*, 18, 4277–4295, 10.5194/acp-18-4277-2018, 2018.

Yang, Y., Wang, Y., Huang, W., Yao, D., Zhao, S., Wang, Y., Ji, D., Zhang, R., and Wang, Y.: Parameterized atmospheric oxidation capacity and speciated OH reactivity over a suburban site in the North China Plain: A comparative study between summer and winter, *Sci Total Environ*, 773, 145264, 10.1016/j.scitotenv.2021.145264, 2021.

Yang, X., Lu, K., Ma, X., Liu, Y., Wang, H., Hu, R., Li, X., Lou, S., Chen, S., Dong, H., Wang, F., Wang, Y., Zhang, G., Li, S., Yang, S., Yang, Y., Kuang, C., Tan, Z., Chen, X., Qiu, P., Zeng, L., Xie, P., and Zhang, Y.: Observations and modeling of OH and HO₂ radicals in Chengdu, China in summer 2019, *Sci Total Environ*, 772, 144829, 2021a 10.1016/j.scitotenv.2020.144829, 2021a.

He, Z., Wang, X., Ling, Z., Zhao, J., Guo, H., Shao, M., and Wang, Z.: Contributions of different anthropogenic volatile organic compound sources to ozone formation at a receptor site in the Pearl River Delta region and its policy implications, *Atmospheric Chemistry and Physics*, 19, 8801-8816, 10.5194/acp-19-8801-2019, 2019.

Li, Z., Xue, L., Yang, X., Zha, Q., Tham, Y. J., Yan, C., Louie, P. K. K., Luk, C. W. Y., Wang, T., and Wang, W.: Oxidizing capacity of the rural atmosphere in Hong Kong, Southern China, *Sci Total Environ*, 612, 1114-1122, 10.1016/j.scitotenv.2017.08.310, 2018.

Suthawaree, J., Kato, S., Okuzawa, K., Kanaya, Y., Pochanart, P., Akimoto, H., Wang, Z., and Kajii, Y.: Measurements of volatile organic compounds in the middle of Central East China during Mount Tai Experiment 2006 (MTX2006): observation of regional background and impact of biomass burning, *Atmos. Chem. Phys.*, 10, 1269–1285, doi:10.5194/acp-10-1269-2010, 2010.

Xue, L. K. , Wang, T. , Guo, H. , Blake, D. R. , Tang, J. , & Zhang, X. C. , et al.: Sources and photochemistry of volatile organic compounds in the remote atmosphere of western China: results from the Mt. Waliguan Observator, *Atmos. Chem. Phys.*, 10.5194/acp-13-8551-2013, 2013.

Hong, Z., Li, M., Wang, H., Xu, L., Hong, Y., Chen, J., Chen, J., Zhang, H., Zhang, Y., Wu, X., Hu, B., and Li, M.: Characteristics of atmospheric volatile organic compounds (VOCs) at a mountainous forest site and two urban sites in the southeast of China, *Sci Total Environ*, 10.1016/j.scitotenv.2018.12.132, 2019.

Zhu, J., Wang, S., Wang, H., Jing, S., Lou, S., Saiz-Lopez, A., and Zhou, B.: Observationally constrained modeling of atmospheric oxidation capacity and photochemical reactivity in Shanghai, China, *Atmos. Chem. Phys.*, 20, 1217-1232, 10.5194/acp-20-1217-2020, 2020.

Xue, L., Gu, R., Wang, T., Wang, X., Saunders, S., Blake, D., Louie, P. K. K., Luk, C. W. Y., Simpson, I., Xu, Z., Wang, Z., Gao, Y., Lee, S., Mellouki, A., and Wang, W.: Oxidative capacity and radical chemistry in the polluted atmosphere of Hong Kong and Pearl River Delta region: analysis of a severe photochemical smog episode, *Atmos. Chem. Phys.*, 16, 9891–9903, 10.5194/acp-16-9891-2016, 2016.